Mycol Progress
DOI 10.1007/s11557-009-0618-0

ORIGINAL ARTICLE

Mycosphaerella podagrariae—a necrotrophic phytopathogen forming a special cellular interaction with its host *Aegopodium podagraria*

Uwe K. Simon · Johannes Z. Groenewald · York-Dieter Stierhof · Pedro W. Crous · Robert Bauer

Received: 3 June 2009 / Revised: 12 August 2009 / Accepted: 14 August 2009

Abstract We present a new kind of cellular interaction found between *Mycosphaerella podagrariae* and *Aegopodium podagraria*, which is remarkably different to the interaction type of the obligate biotrophic fungus *Cymadothea trifolii*, another member of the Mycosphaerellaceae (Capnodiales, Dothideomycetes, Ascomycota) which we have described earlier. Observations are based on both conventional and cryofixed material and show that some features of this particular interaction are better discernable after chemical fixation. We were also able to generate sequences for nuclear ribosomal DNA (complete SSU, 5.8 S and flanking ITS-regions, D1–D3 region of the LSU) confirming the position of *M. podagrariae* within Mycosphaerellaceae.

U. K. Simon (✉)
Institut für Pflanzenwissenschaften,
Universität Graz,
Schubertstraße 51,
A-8010 Graz, Austria
e-mail: uwe.simon@uni-graz.at

J. Z. Groenewald · P. W. Crous
Fungal Biodiversity Centre,
Centraalbureau voor Schimmelcultures,
P.O. Box 85167, 3508 AD Utrecht, The Netherlands

Y.-D. Stierhof
Zentrum für Molekularbiologie der Pflanzen,
Universität Tübingen,
Auf der Morgenstelle 5,
72076 Tübingen, Germany

R. Bauer
Lehrstuhl Spezielle Botanik, Universität Tübingen,
Auf der Morgenstelle 1,
72076 Tübingen, Germany

Keywords Dothideomycetes · ITS · LSU · Molecular phylogeny · SSU

Introduction

Mycosphaerellaceae (Capnodiales, Dothideomycetes) is one of the most species-rich groups of ascomycotan fungi, containing species that are saprobic, endophytic, biotrophic, nectrotrophic, and hemibiotrophic (Verkley et al. 2004; Aptroot 2006; Crous et al. 2006). Recent DNA phylogenetic studies using the nuclear ribosomal RNA operon as well as house-keeping genes have revealed its extreme genetic diversity (Arzanlou et al. 2007; Crous et al. 2007a, b). In spite of the size and economic importance of the Mycosphaerellaceae, cellular interactions of this family with various host plants are still poorly documented. However, Simon et al. (2004) described a very intricate interaction between the obligate biotrophic sooty blotch disease of clover *Cymadothea trifolii* (= *Mycosphaerella killiani*) and its *Trifolium* host species. There, the fungus forms a highly complex interaction apparatus in its own hyphae opposite to which the plant plasma membrane invaginates to form a bubble. Both structures are linked by a tube of electron dense material leading through the cell walls of either organism. Within the tube, the plant cell wall is partially but not totally degraded as shown by Simon et al. (2005a). The plant cell reacts by applying cell wall appositional material onto the site of interaction, which, consequently, comes to an end. Both pathogen and host cell survive and the whole process may be repeated, or other plant cells may be attacked. Here, we report the cellular interaction between the necrotrophic *Mycosphaerella podagrariae* and *Aegopodium podagraria* using both chemically and cryofixed infected plant material. To determine the

Published online: 19 September 2009

phylogenetic position of this fungus, we sequenced the complete small subunit (SSU; 18S nrDNA), the complete internal transcribed spacer regions including the 5.8S nrRNA gene (ITS), and the D1-D3 region of the large subunit (LSU; 28S nrDNA) of the nuclear ribosomal DNA operon. See Table 1 for details of fungal strains used in this study.

Materials and methods

Fungus material

Material used in this study was collected from:

Germany: Baden-Württemberg: Kirnbachtal (near Bebenhausen/Tübingen), on *Aegopodium podagraria*, July 2007, Herbarium TUB 019186.

Fixation, sectioning of resin-embedded material, post-staining and TEM analysis Chemical and cryofixation as well as freeze-substitution, sectioning, post-staining and TEM analysis with a ZEISS EM 109 at 80 kV was done as described by Simon et al. (2005b). Interaction sites were scrutinized via serial sectioning, and at least 100 interactions sites were studied.

DNA extraction and amplification

DNA extraction was performed using the DNAeasy Plant Mini Kit (Qiagen, Hilden, Germany) according to the manufacturer's instructions after mechanically breaking up cell walls with a mixer mill. Polymerase chain reactions (PCR) were performed in a total volume of 50 µl containing 5 µL 10× PCR-buffer (Life Technologies, Eggenstein, Germany), 34.1 µL H_2O, 2 µl $MgCl_2$ (50 mM stock; Life Technologies), 2 µL dNTPs (5 mM stock; Life Technologies), 1 µL forward and 1 µL reverse primers (25 pmol/µl stock each), 0.2 µL Bovine Serum Albumin (BSA; Sigma-Aldrich, Munich, Germany, 1 % stock), 0.2 µL *Taq* polymerase (5 units/µL stock; Life Technologies) and 5 µL DNA extract diluted 1:10. The following primers were used for amplification: SSU: NS17 - NS24 (Gargas and Taylor 1992); ITS: V9G (de Hoog and Gerrits van den Ende 1998) and ITS 4 (White et al. 1990); LSU: LROR and LR5 (Vilgalys and Hester 1990). Amplifications were carried out on a thermal cycler (Applied Biosystems) equipped with a heated lid. PCR parameters were as follows: 35 cycles with initial denaturation at 94°C for 5 min followed by 30 s at 94°C, 90 s at either 45, 50, 55°C, or 60°C (depending on primers), 4 min at 72°C, plus a final 7-min extension at 72°C with subsequent cooling down to 4°C.

Table 1 Species names, culture collection and GenBank accession numbers of fungal strains used in this study. The GenBank accession number is for the concatenated 18S nrDNA, ITS1, 5.8S nrDNA, ITS2 and partial 28S nrDNA sequence. *Mycosphaerella podagrariae* is indicated in bold

Species	Strain no.[a]	GenBank no.[b]
Ascochyta fabae	CBS 114.36	EU167566
Ascochyta viciae-villosae	CBS 255.92	EU167560
Asteroma alneum	CBS 109840	EU167609
Bagnisiella examinans	CBS 551.66	EU167562
Davidiella macrospora	CBS 138.40	EU167591
Davidiella tassiana	CBS 723.79	EU167558
Didymella bryoniae	CBS 233.52	EU167573
Didymella exitialis	CBS 446.82	EU167564
Dothidea berberidis	CBS 186.58	EU167601
Dothidea muelleri	CBS 191.58	EU167593
Guignardia vaccinii	CBS 114751	EU167584
Kabatiella caulivora	CBS 242.64	EU167576
Kabatiella microsticta	CBS 342.66	EU167608
Mycosphaerella aleuritidis	CBS 282.62	EU167594
Mycosphaerella arbuticola	CBS 355.86	EU167571
Mycosphaerella berberidis	CBS 324.52	EU167603
Mycosphaerella brassicicola	CBS 174.88	EU167607
Mycosphaerella coacervata	CBS 113391	EU167596
Mycosphaerella crystallina	CBS 681.95	EU167579
Mycosphaerella flageoletiana	CBS 114302	EU167597
Mycosphaerella fragariae	CBS 719.84	EU167604
Mycosphaerella gregaria	CBS 110501	EU167580
Mycosphaerella grossulariae	CBS 235.37	EU167588
Mycosphaerella handelii	CBS 113302	EU167581
Mycosphaerella harthensis	CBS 325.52	EU167602
Mycosphaerella laricina	CBS 326.52	EU167595
Mycosphaerella linorum	CBS 261.39	EU167590
Mycosphaerella microsora	CBS 100352	EU167599
Mycosphaerella milleri	CBS 541.63	EU167577
Mycosphaerella podagrariae	**TUB 019186**	**EU386700**
Mycosphaerella populicola	CBS 100042	EU167579
Mycosphaerella pseudoellipsoidea	CBS 114709	EU167585
Mycosphaerella punctata	CBS 113315	EU167582
Mycosphaerella punctiformis	CBS 113265	EU167569
Mycosphaerella pyri	CBS 100.86	EU167606
Mycosphaerella rosigena	CBS 330.51	EU167586
Mycosphaerella rubi	CBS 238.37	EU167589
Mycosphaerella stromatosa	CBS 101953	EU167598
Phoma exigua var. *exigua*	CBS 118.94	EU167567
Phoma sojicola	CBS 567.97	EU167568
Pleiochaeta setosa	CBS 496.63	EU167563
Teratosphaeria microspora	CBS 101951	EU167572
Teratosphaeria molleriana	CBS 118359	EU167582

[a] *CBS* CBS Fungal Biodiversity Centre, Utrecht, The Netherlands

[b] All sequences used in this work apart from those of *M. podagrariae* were obtained during our previous study (Simon et al. 2009)

Sequencing

For cycle sequencing the same primers were applied as for PCR using the ABI PRISM Dye-Terminator Cycle Sequencing Kit v. 3.1 (Applied Biosystems) according to the manufacturer's protocol, but with a reaction volume of 10 μL and the enzyme diluted 1:6 with the supplied dilution buffer. Electrophoresis and data sampling were performed on an automated sequencer (ABI 3100; Applied Biosystems). Sequences were manually edited with SEQUENCHER™ v. 4.1.2 (Gene Codes Corporation, Ann Arbor, Mi, USA).

Phylogenetic analyses

Concatenated SSU, ITS, and LSU sequences were automatically aligned using MAFFT v. 6.240 (Katoh et al. 2002; Katoh and Toh 2007). The Mafft alignment was subsequently treated with Gblocks v. 0.91b (Castresana 2000) using the -b5=h option to only retain positions with gaps in up to half of the sequences. To estimate phylogenetic relationships alignments were analysed with (1) BIONJ (Gascuel 1997) as implemented in PAUP v. 4.0b10 (Swofford 2003) using the TamNei+I+G substitution model as suggested by Modeltest v. 3.6 (Posada and Crandall 1998) and ties broken taxon-order dependently; (2) heuristic maximum likelihood (ML) analysis as implemented in RAxML (Stamatakis 2006) using the GTRMIX substitution model and 100 independent heuristic searches combined with a ML bootstrap analysis (1,000 bootstrap replicates); and (3) with a Bayesian Markov chain Monte Carlo (MCMC) approach as implemented in MrBayes v. 3.1.2 (Ronquist and Huelsenbeck 2003) with two independent runs of four incrementally heated simulta-

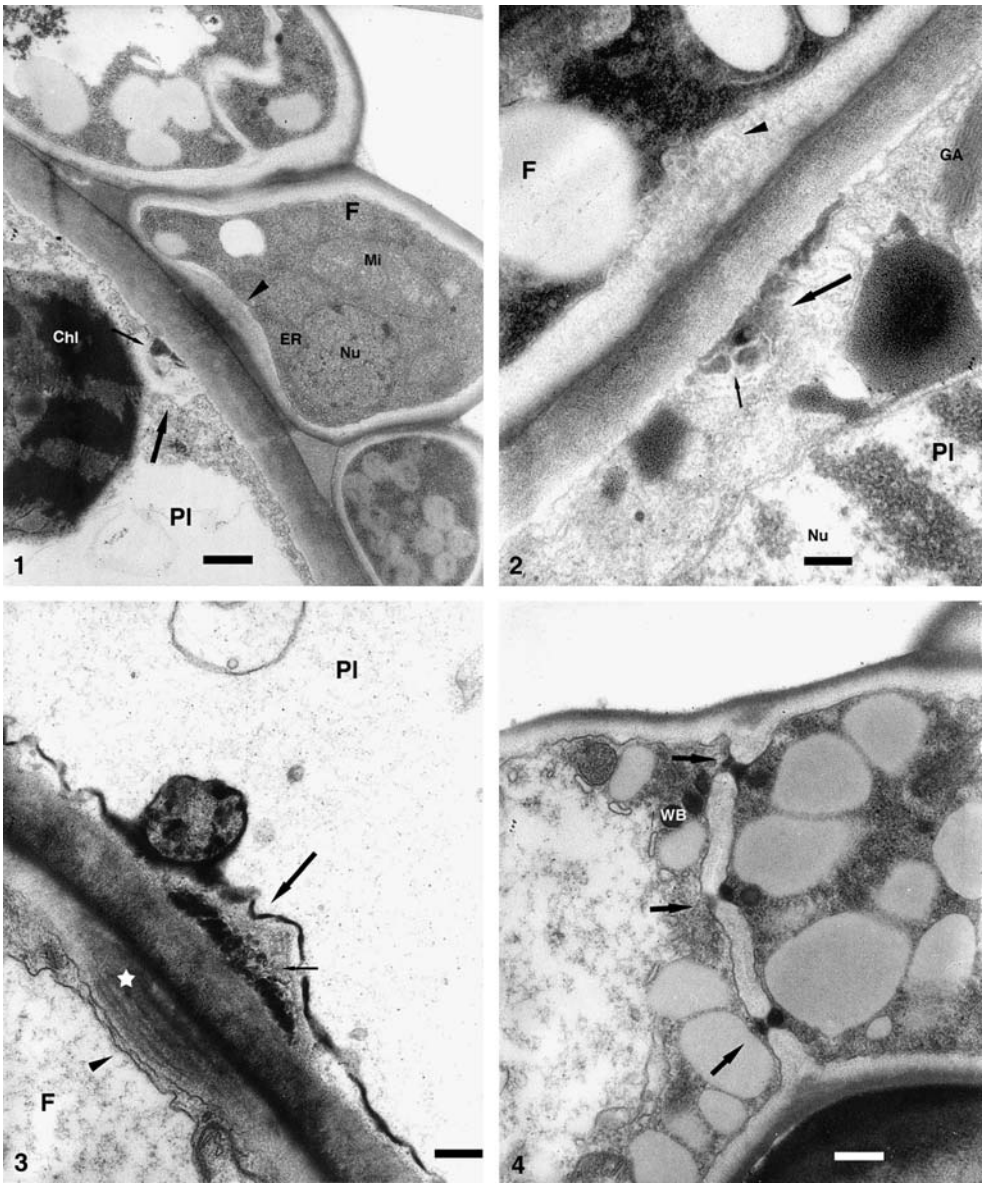

Fig. 1 Chemically fixed samples of *Aegopodium podagraria* leaves infected with *M. podagrariae*. *1, 2* Early stages of the interaction. Partly electron opaque material is applied onto the host wall opposite to a localized thickening of the fungal wall from which some electron dense substance seems to be secreted. The plant cell appears to be still healthy as indicated by well-preserved organelles such as chloroplasts and Golgi apparatus. *Bars 1* 0.5 μm, *2* 0.2 μm. *3* The plant cell is visibly degenerated. Much more and darker electron dense substance is found at the interaction site and both in and secreted from the pathogen wall (*star*). *Bar* 0.2 μm. *4* Septum of *M. podagrariae* with 3 pores (*medium-sized arrows*) plugged with Woronin bodies. *Bar* 0.5 μm. *Chl* Chloroplast, *ER* endoplasmic reticulum, *F* fungus, *GA* Golgi apparatus, *Mi* mitochondrion, *Nu* nucleus, *Pl* plant, *WB* Woronin body; *large arrows* point at material appositioned onto the plant cell wall, *small arrows* at electron dense substance within the latter, and *arrowheads* at fungal cell wall thickenings

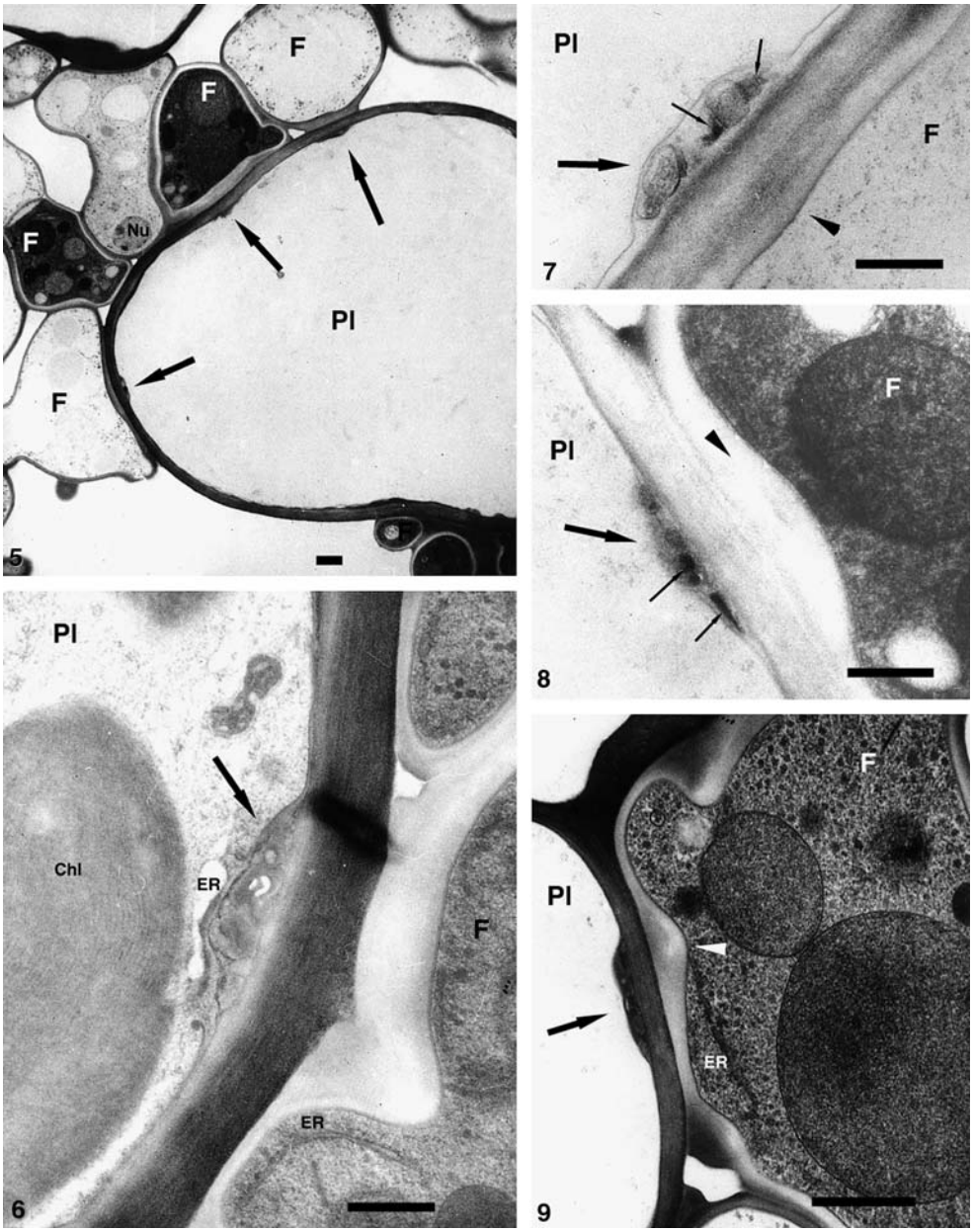

Fig. 2 Cryofixed samples of *A. podagraria* leaves infected with *M. podagrariae*. *5* A killed host cell which had been attacked by several hyphae as shown by interaction sites. *Bar* 1 μm. *6* Early stage of interaction. Organelles such as chloroplasts and endoplasmic reticulum are well preserved. The material applied onto the plant cell wall during the interaction appears free of the electron dense substance. *Bar* 0.5 μm. *7* Later stage of interaction. Applied material includes large vacuoles and some electron dense substance which is also present to a lesser degree in the opposite cell wall area of the pathogen. *Bar* 0.5 μm. *8, 9* Most (*8*), finally all (*9*) of the cell wall appositional material in the plant cell is now filled with the electron dense substance. *Bars* 8 0.5 μm, 9 1 μm. *Chl* Chloroplast, *ER* endoplasmic reticulum, *F* fungus, *GA* Golgi apparatus, *Mi* mitochondrion, *Nu* nucleus, *Pl* plant, *WB* Woronin body; *large arrows* point at material appositioned onto the plant cell wall, *small arrows* at electron dense substance within the latter, and *arrowheads* at fungal cell wall thickenings

neous Monte Carlo Markov chains each over four million generations using random starting trees and the GTR+I+G substitution model (Huelsenbeck and Rannala 2004). Model parameters were sampled during MCMC. Trees were acquired every 100 generations resulting in 40,000 trees per run, from which the first 10,000 of each run were discarded (burn in). The remaining 60,000 trees (twice 30,000) were pooled and a majority rule consensus tree was computed to get estimates for the posterior probabilities. Stationarity of the process was assessed using Tracer v. 3.1 (Rambaut and Drummond 2003). All sequences except those of *M. podagrariae* were obtained in an earlier study (Simon et al. 2009). Trees were rooted with *Asteroma alneum* (Sordariomycetes) as outgroup taxon.

Results

Electron microscopy

Both heavily and less severely infected leaf areas were analyzed (Figs. 1 and 2), but no difference in the

Fig. 3 BIONJ tree of an alignment of complete nuclear ribosomal SSU, complete ITS, and partial LSU (D1-D3) sequences for *M. podagrariae* and 42 additionally species based on the TamNei+G+I substitution model. The tree was rooted with *Asteroma alneum* as outgroup species. *Numbers* on *branches* denote bootstrap support values (values below 50% were omitted). The relevant order and class names are given on the *right* with family designations included for Capnodiales. *Botryosph.* Botryosphaeriales, *D* Dothideomycetes, *S* Sordariomycetes

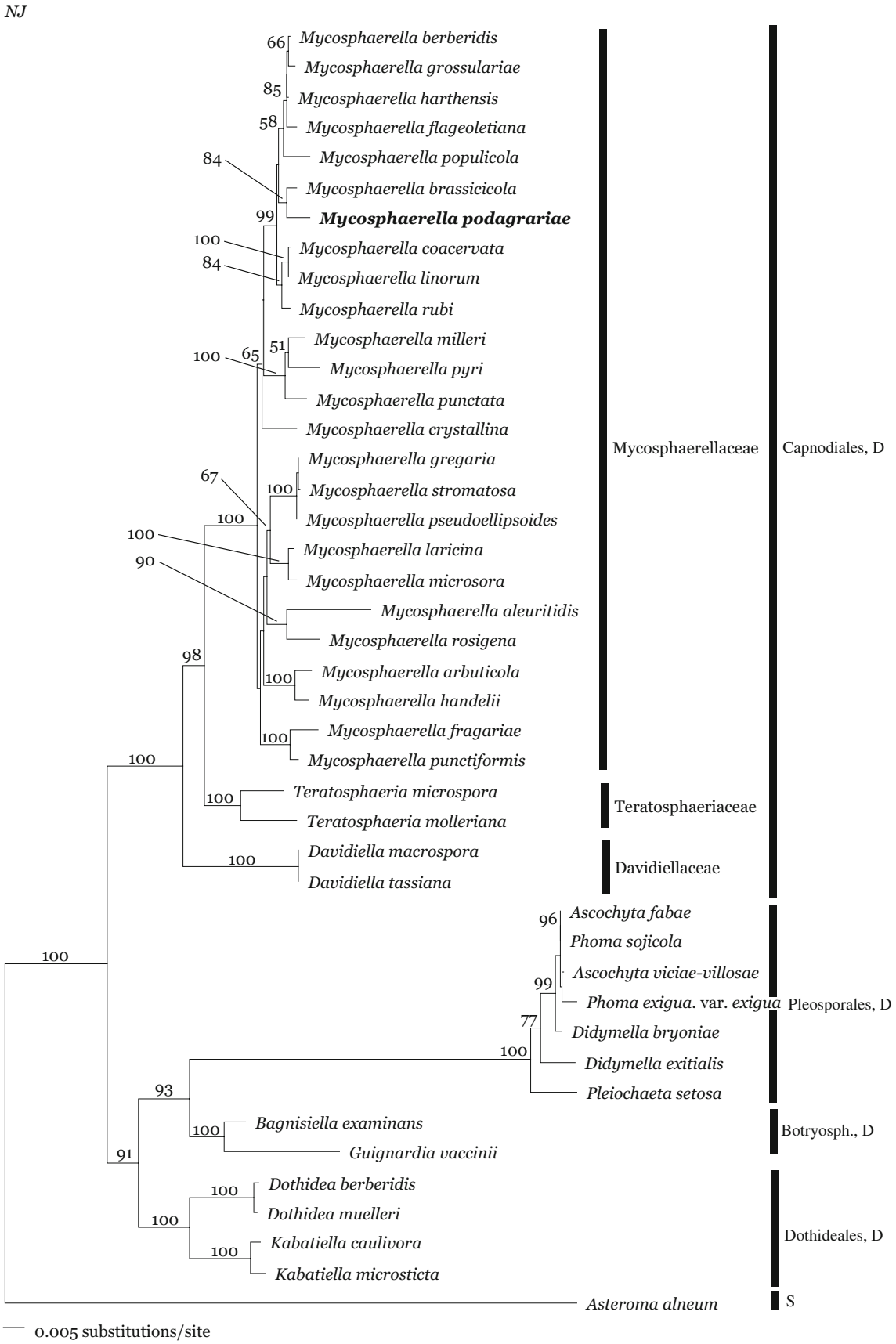
NJ
Mycosphaerella berberidis
Mycosphaerella grossulariae
Mycosphaerella harthensis
Mycosphaerella flageoletiana
Mycosphaerella populicola
Mycosphaerella brassicicola
Mycosphaerella podagrariae
Mycosphaerella coacervata
Mycosphaerella linorum
Mycosphaerella rubi
Mycosphaerella milleri
Mycosphaerella pyri
Mycosphaerella punctata
Mycosphaerella crystallina
Mycosphaerella gregaria
Mycosphaerella stromatosa
Mycosphaerella pseudoellipsoides
Mycosphaerella laricina
Mycosphaerella microsora
Mycosphaerella aleuritidis
Mycosphaerella rosigena
Mycosphaerella arbuticola
Mycosphaerella handelii
Mycosphaerella fragariae
Mycosphaerella punctiformis
Teratosphaeria microspora
Teratosphaeria molleriana
Davidiella macrospora
Davidiella tassiana
Ascochyta fabae
Phoma sojicola
Ascochyta viciae-villosae
Phoma exigua. var. exigua
Didymella bryoniae
Didymella exitialis
Pleiochaeta setosa
Bagnisiella examinans
Guignardia vaccinii
Dothidea berberidis
Dothidea muelleri
Kabatiella caulivora
Kabatiella microsticta
Asteroma alneum
Mycosphaerellaceae
Teratosphaeriaceae
Davidiellaceae
Capnodiales, D
Pleosporales, D
Botryosph., D
Dothideales, D
S
0.005 substitutions/site

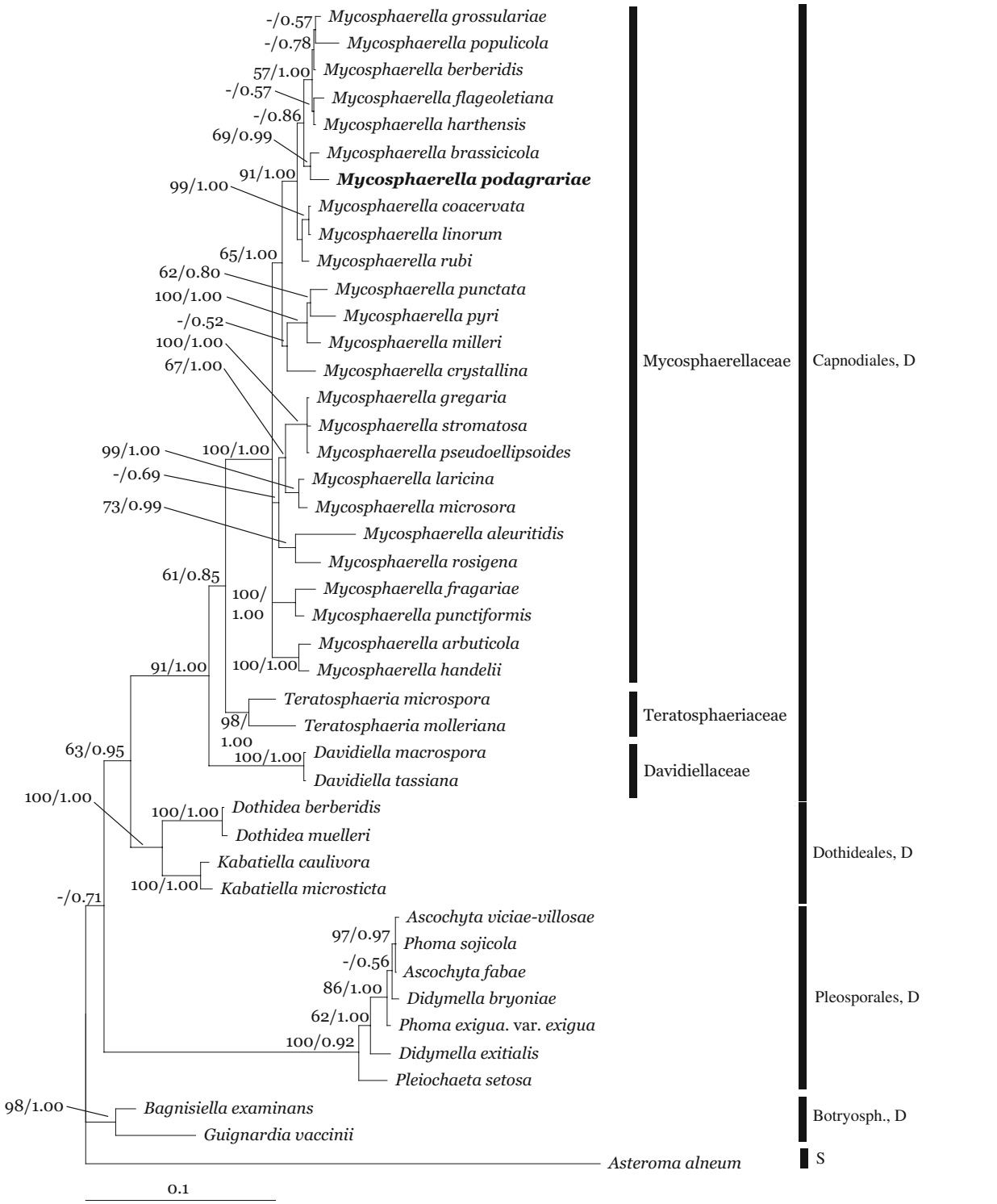

Fig. 4 Phylogenetic tree based on heuristic maximum likelihood analyses. *Numbers* on *branches* designate maximum likelihood bootstrap values (left) and MCMC estimates of posterior probabilities (*right* values below 0.5 were omitted). Abbreviations as in Fig. 3

appearance of the cellular interaction could be observed. In apparently earlier stages of infection, when plant cells seemed still intact, the interaction was characterized by a slightly increased thickness of the pathogen cell wall and, opposite to it, accumulation of membranous material onto the host cell wall, including some electron dense substance (Figs. 1 parts 1, 2, and 2 parts 6, 7). In later stages (Figs. 1 part 3, and 2 parts 5, 8, 9) these membranes were difficult to discriminate and the electron dense substance made up a large proportion of the material applied onto the plant cell wall. In chemically fixed samples we could find a few interaction sites where the wall of the fungus contained and/or secreted an electron dense substance (Fig. 1 parts 1, 3). This phenomenon was less pronounced in cryofixed samples, but found here as well (Fig. 2 part 7). In both plant and fungal cells, nuclei and endoplasmic reticulum (ER) were usually close to the site of interaction (Figs. 1 parts 1, 2, and 2 part 6). As seen in Fig. 2 part 5, one plant cell could be attacked by several hyphae of the pathogen. We never observed instances of the fungus entering a host cell. Figure 1 part 4 shows a multipored septum of the fungus with Woronin bodies as pore plugs.

Phylogenetic analyses

All phylogenetic algorithms produced similar tree topologies for Mycosphaerellaceae (Figs. 3 and 4). Although this family as such was well supported, some subgroups showed little or no support or appeared paraphyletic. However, all three methods clearly placed *M. podagrariae* in Mycosphaerellaceae with *M. brassicicola* as nearest relative. Interestingly, Dothideales were either placed in a sister relationship to Botryosphaeriales/Pleosporales (NJ; Fig. 3), or to Capnodiales (RaXML/MCMC, Fig. 4).

Discussion

The interaction between *M. podagrariae* and *A. podagraria* is remarkable in that it is the first of its kind in Dothideomycetes characterized by accumulation of material onto the cell walls of both organisms. An increasing amount of an unknown electron dense substance is integrated into the material applied onto the host wall. The host cell seems to get killed by the fungus (finally, most of the leaf area is necrotic; not shown), though the mechanism behind this remains currently not understood. However, toxins could be involved in this process as speculated for *M. graminicola* (Palmer and Skinner 2002). With respect to the electron dense substance detected in interaction zones, it is difficult to decide whether it is of fungal origin as observed by Bauer et al. (1995) for *Ustacystis waldsteiniae*, or a defense reaction of the attacked plant cell, or both. The proximity of nuclei and ER to the site of interaction in pathogen and plant cell at least indicates high metabolic activity at this location. It is noteworthy that the same host cell can be attacked by several hyphae as is the case for *Trifolium repens* leaves infected with *C. trifolii* (Simon et al. 2005b). Both *C. trifolii* and *M. podagrariae* never invade the plant cell itself. However, in contrast to the first, which is an obligate biotrophic pathogen, *M. podagrariae* kills the host cell.

The comparison of two embedding techniques shows that chemical fixation may elucidate features less evident after cryofixation, although structural preservation is much better in the latter method. However, the electron dense substance present in the wall appositional material in the plant cell and, to a lesser degree, in the fungal wall was much easier to detect in chemically fixed samples, probably because of the stronger contraction of material during this kind of fixation. Therefore, both techniques may have their value in the study of plant–pathogen interactions.

We were also able to obtain genetic information for this fungus which has not been sequenced until now. Phylogenetic results based on sequencing the complete SSU and ITS region, and the D1–D3 region of the LSU produced conflicting results for the position of Dothideales, grouping them either with Botryosphaeriales/Pleosporales or with Capnodiales. Taking into account the data obtained by Schoch et al. (2006), who additionally used protein-coding genes for their phylogenies, the latter is more likely to reflect true relationships. Nevertheless, all topologies unequivocally show that *M. podagrariae* is a true member of Mycosphaerellaceae s.str. However, it is clearly not closely related to *C. trifolii*, which groups with *M. rosigena* and *M. aleuritidis* (Simon et al. 2009), but has not been included in the present study because we failed to obtain ITS sequences for this pathogen. Instead, it clustered with *M. brassicicola* in all three phylogenetic algorithms applied. This further strengthens our hypothesis that different life strategies within Mycosphaerellaceae—probably mirrored by specific types of cellular interaction—may form separate clusters within this family (Simon et al. 2009).

Acknowledgements We are grateful to Heinz Schwarz, Max-Planck-Institute for Developmental Biology, Tübingen, Germany, for help with cryofixation. U.K.S. was funded by the German Research Foundation (DFG). We thank two anonymous reviewers for their critical reading and valuable suggestions.

References

Aptroot A (2006) *Mycosphaerella* and its Anamorphs: 2. Conspectus of Mycosphaerella. CBS Biodiversity Series 5, Utrecht, The Netherlands

Arzanlou M, Groenewald JZ, Gams W, Braun U, Shin H-D, Crous PW (2007) Phylogenetic and morphotaxonomic revision of *Ramichloridium* and allied genera. Stud Mycol 58:57–93

Bauer R, Mendgen K, Oberwinkler F (1995) Cellular interaction of the smut fungus *Ustacystis waldsteiniae*. Can J Bot 73:867–883

Castresana J (2000) Selection of conserved blocks from multiple alignments for their use in phylogenetic analysis. Mol Bio Evol 17:540–552

Crous PW, Wingfield MJ, Mansilla JP, Alfenas AC, Groenewald JZ (2006) Phylogenetic reassessment of *Mycosphaerella* spp. and their anamorphs occurring on *Eucalyptus*. II. Stud Mycol 55:99–131

Crous PW, Braun U, Groenewald JZ (2007a) *Mycosphaerella* is polyphyletic. Stud Mycol 58:1–32

Crous PW, Braun U, Schubert K, Groenewald JZ (2007b) Delimiting *Cladosporium* from morphologically similar genera. Stud Mycol 58:33–56

Gargas A, Taylor JW (1992) Polymerase chain reaction (PCR) primers for amplifying and sequencing nuclear 18S rDNA from lichenized fungi. Mycologia 84:589–592

Gascuel O (1997) BIONJ: an improved version of the NJ algorithm based on a simple model of sequence data. Mol Bio Evol 14:685–695

de Hoog GS, Gerrits van den Ende AHG (1998) Molecular diagnostics of clinical strains of filamentous Basidiomycetes. Mycoses 41:183–189

Huelsenbeck JP, Rannala B (2004) Frequentist properties of Bayesian posterior probabilities of phylogenetic trees undersimple and complex substitution models. Sys Biol 53:904–913

Katoh K, Toh H (2007) PartTree: an algorithm to build an approximate tree from a large number of unaligned sequences. Bioinformatics 23:372–374

Katoh K, Misawa K, Kuma KI, Miyata T (2002) MAFFT: a novel method for rapid multiple sequence alignment based on fast Fourier transform. Nucl Acids Res 30:3059–3066

Palmer C-L, Skinner W (2002) *Mycosphaerella graminicola*: latent infection, crop devastation and genomics. Mol Plant Pathol 3 (2):63–70

Posada D, Crandall KA (1998) Modeltest: testing the model of DNA substitution. Bioinformatics 14:817–818

Rambaut A, Drummond A (2003) Tracer MCMC trace analysis tool, version 1.3. University of Oxford, Oxford, UK. [http://tree.bio.ed.ac.uk/software/tracer/]

Ronquist F, Huelsenbeck JP (2003) MrBayes 3: Baysian phylogenetic inference under mixed models. Bioinformatics 19:1572–1574

Schoch CL, Shoemaker RA, Seifert KA, Hambleton S, Spatafora JW, Crous PW (2006) A multigene phylogeny of the Dothideomycetes using four nuclear loci. Mycologia 98:1041–1052

Simon UK, Bauer R, Oberwinkler F (2004) The unique cellular interaction between the leaf pathogen *Cymadothea trifolii* and *Trifolium repens*. Mycologia 96:1210–1218

Simon UK, Bauer R, Rioux D, Simard M, Oberwinkler F (2005a) The intercellular biotrophic leaf pathogen *Cymadothea trifolii* locally degrades pectins, but not cellulose or xyloglucan in the cell walls of *Trifolium repens*. New Phytol 165:243–260

Simon UK, Bauer R, Rioux D, Simard M, Oberwinkler F (2005b) The vegetative life cycle of the clover pathogen *Cymadothea trifolii* as seen in the electron microscope. Mycol Res 109:764–778

Simon UK, Groenewald JZ, Crous PW (2009) *Cymadothea trifolii*, an obligate biotrophic parasite of *Trifolium*, belongs to the Mycosphaerellaceae as shown by nuclear ribosomal DNA analyses. Persoonia 22:49–55

Stamatakis A (2006) RAxML-VI-HPC: maximum likelihood-based phylogenetic analyses with thousands of taxa and mixed models. Bioinformatics 22:2688–2690

Swofford DL (2003) PAUP*. Phylogenetic analysis using parsimony (*and other methods). Version 4. Sinauer Associates, Sunderland, MA, USA

Verkley GJM, Crous PW, Groenewald JZ, Braun U, Aptroot A (2004) *Mycosphaerella punctiformis* revisited: morphology, phylogeny, and epitypification of the type species of the genus *Mycosphaerella* (Dothideales, Ascomycota). Mycol Res 108:1271–1282

Vilgalys R, Hester M (1990) Rapid genetic identification and mapping of enzymatically amplified ribosomal DNA from several *Cryptococcus* species. J Bacteriol 172:4238–4246

White TJ, Bruns T, Lee S, Taylor J (1990) Amplification and direct sequencing of fungal ribosomal RNA genes for phylogenetics. In: Innis MA, Gelfand DH, Sninsky JJ, White TJ (eds) PCR protocols: a guide to methods and applications. Academic, San Diego, pp 315–322